REINFORCEMENT OF EXISTING DEEP FOUNDATIONS WITH MICROPILES

Freddy Lopez[1], Jann-Eike Saathoff[2], Martin Achmus[3]

ABSTRACT

Several structures (bridges, industrial facilities, etc.) are built on piled foundations. In many cases, the existing structures and their foundations need to be reinforced or retrofitted, because the original use of these structures has been subjected to changes that require increased load bearing capacities (e.g. former industrial facilities are reused for housing), or because the serviceability needs to be enhanced, even though the original use remains the same. The latter is a common case when national building codes are updated or when the structures behave differently as originally planned (i.e. unacceptable settlements).
It is certainly common to undertake the retrofitting works from the existing foundation levels, with the corresponding space restrictions (limited working heights). Under these conditions, the use of micropiles has enabled designers to come up with technical feasible solutions to retrofit the existing deep foundations, making the structural reinforcement a real option, even under considerable changes in the loading conditions.
The present article describes a proposed reinforcement of existing cast-in-place bored piles with a group of self-drilling micropiles, to increase the load-bearing capacity of the original deep foundation. This paper will focus mainly on the analysis of the interaction between the existing piles and the reinforcing micropiles. A parametric study with a variation of the geotechnical parameters of the underground to obtain the optimal reinforcement configuration will be carried out.

1. SI CONVERSION FACTORS

Table 1. Approximate conversions from SI Units

Dimension	Symbol	When you know	Multiply by	To Find	Symbol
Length	cm	centimeters	0.394	inches	in
	m	meters	3.281	feet	ft
Force	kN	kilonewtons	224.81	poundforce	lbf
	MN	meganewtons	224.81	kilopoundforce	kip
Pressure	Bar	bars	0.01	kilopoundforce/square inch	ksi
Stresses	kPa (kN/m^2)	kilopascals	0.145	Poundforce/square inch	psi
	MPa (MN/m^2)	megapascals	145	Poundforce/square inch	psi

2. INTRODUCTION

During the feasibility study of an intervention project in the city of Cologne, Germany, the reinforcement of an existing deep foundation -consisting of cast-in-place bored piles or drilled shafts- with self-drilling micropiles was proposed.

[1] MSc.-Ing, Friedr. Ischebeck GmbH, Loher Str. 31-79 / 58256 Ennepetal (GER), lopez@ischebeck.de
[2] MSc.-Ing, Institut für Geotechnik – Leibniz Universität Hannover, Appelstr. 9A/ 30167 Hannover (GER), saathoff@igth.uni-hannover.de
[3] Univ. Prof. Dr.-Ing, Institut für Geotechnik – Leibniz Universität Hannover, Appelstr. 9A/30167 Hannover (GER), achmus@igth.uni-hannover.de

Self-drilling micropiles consist of continuously threaded hollow bars, made of seamless steel pipes, installed via rotary percussive drilling. During the drilling process, the micropiles are continuously grouted (dynamic injection), building a rough interlocking at the interface grout-soil, increasing the skin friction (Lopez and Fernandez, 2017). The use of self-drilling micropiles has been proven to be a very versatile and cost-effective solution and is increasingly implemented in different intervention projects, both for the construction of new infrastructure and as reinforcement to retrofit existing structures. These piles can be installed using very flexible drilling equipment, enabling the assembly of long micropiles even in confined spaces and obtaining high drilling performances associated to very low vibrations (Lopez and Severi, 2017).
For the analysis of the reinforced foundation, a numerical model was developed at the Institute for Geotechnical Engineering (IGtH) of the Leibniz University of Hannover, Germany. The conducted analysis and the obtained results were described in a technical paper, presented at the 43rd DFI Annual Conference in Anaheim, USA (Lopez et al., 2018).
After receiving updated information regarding the actual pile geometry and loading conditions, a second analysis of the existing and reinforced foundations was conducted. Based on the obtained results, additional analyses were carried out to evaluate the response of the retrofitted foundation under different ground conditions. The following document presents the results of the parametric study, including the updated analysis of the original study case, the intervention project “Aggripabad” in Cologne, Germany.

The scope of the intervention involved the reuse of a two-story parking deck (with one underground level) to house an extension of the attached five-story building, a public indoor swimming pool. According to the updated information provided by the structural engineer, the existing parking decks are founded on 9.0 m-long cast-in-place bored piles (**D = 0.8 m**), which were designed in 1999 for a compressive service load of $\mathbf{N_{serv,0} = 1000\ kN}$ according to the German Standards DIN 1054 and DIN 4014, valid at that time. Due to the extension of the facilities, it is expected that the existing piles will be loaded with a new service (characteristic) load of $\mathbf{N_{serv,1} = 2500\ kN}$, resulting in a load increment of $\mathbf{\Delta N_{serv} = 1500\ kN}$. Due to the considerable load increase, it was expected that the existing piles could not fulfill the new load requirements without additional reinforcement. Therefore, retrofitting measures using self-drilling micropiles were presented to the Structural Engineers in the scope of a feasibility study. An overview of the planned intervention and the proposed reinforcement is presented in Fig. 1. The optimal angle of the piles was derived in a preliminary analysis to be 15°.

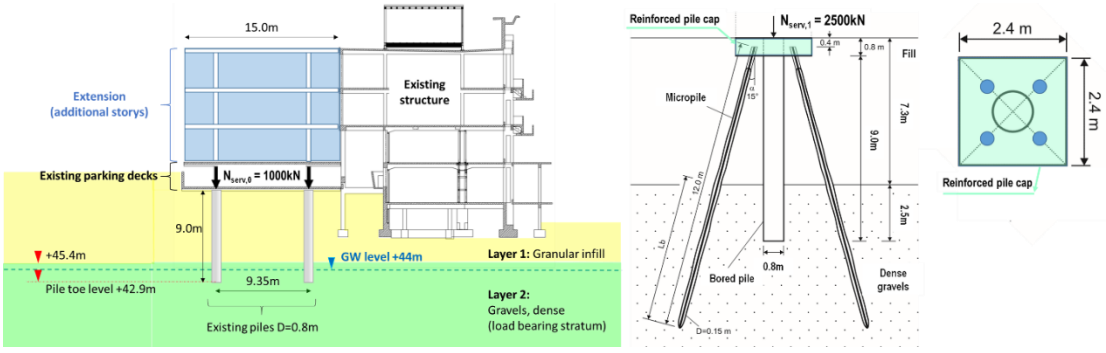

Fig. 1. Intervention project and proposed reinforcement (after Lopez et al., 2018)

3. ANALYSIS OF THE REINFORCED FOUNDATION

There is no analytical model to evaluate the interaction between the existing piles and the proposed reinforcement, therefore the evaluation was carried out with a three-dimensional numerical model of the reinforced pile foundation system, using the finite element program PLAXIS3D (Brinkgreve et al., 2018). Preliminary analyses focused on evaluating the load bearing behavior of the single piles, comparing the results of the numerical simulation with the results of an analytical model described in the book "Recommendations on Piling (EAP)" (DGGT, 2012), which in combination with the Eurocode 7 (EN 1997-1, 2010) depicts the current German practice for the design of piled foundations.
After calibrating the numerical models to simulate the behavior of the single piles, the interaction between the elements of the reinforced foundation (pile and micropiles) was evaluated. In the following sections, both the analytical model of the EAP and the numerical model will be briefly described.

3.1 The EAP-analytical model (DGGT, 2012).

According to the "Recommendations on Piling (EAP)", the characteristic pile resistance ($R_{c,k}$) of bored piles (drilled shafts) can be obtained from the tip or base resistance ($R_{b,k}$) and the shaft resistance ($R_{s,k}$):

$$R_{c,k} = R_{b,k} + R_{s,k} \quad [1]$$

$$R_{b,k} = \frac{\pi}{4} * D^2 * q_{b,k} \quad [2]$$

$$R_{s,k} = \pi * D * \sum(q_{s,ki} * L_i) \quad [3]$$

Here D is the pile diameter and L_i is the thickness of the i-th soil layer around the pile. Both the characteristic base pressure $q_{b,k}$ and the skin friction $q_{s,k}$ are tabulated in the EAP dependent on soil type (non-cohesive or cohesive), soil strength (described by the CPT cone resistance q_c for non-cohesive or by the undrained shear strength $c_{u,k}$ for cohesive soils) and pile settlement (s). For the base pressure ($q_{b,k}$), values are given for settlements corresponding to 2%, 3% and 10% of the pile diameter (D). For the skin friction ($q_{s,ki}$), a linear increase with settlement is assumed until the maximum skin friction is reached at a limit settlement value (s_{sg}):

$$s_{s,g} = 5x10^{-4} * R_{s,k\,(s_{s,g})}\ [in\ kN] + 0.5\ cm \leq 3cm \quad [4]$$

It is worth mentioning that the EAP-values base on extensive, calibrated databases for different pile systems. Empirical values not only for bored piles, but also for micropiles are available in the EAP.

3.2 The numerical model (single pile simulation)

Although the single pile system is axisymmetric, a 3D model was established in order to enable the analysis of the reinforcement by micropiles in a subsequent step. However, due to the symmetry conditions of the loading and the pile-soil system, only one quarter of the system had to be modeled in order to reduce computational effort.
By means of preliminary analyses sufficient mesh fineness with regard to solution accuracy was found and the model dimensions were chosen to avoid any impact of the boundary conditions. The final model is discretized with roughly 220,000 elements and has a width and breadth of 15-times the pile diameter (**D**) and a depth

of 2-times the pile length (**L**). The mesh of the finite element model and its geometry are presented in Fig. 2.

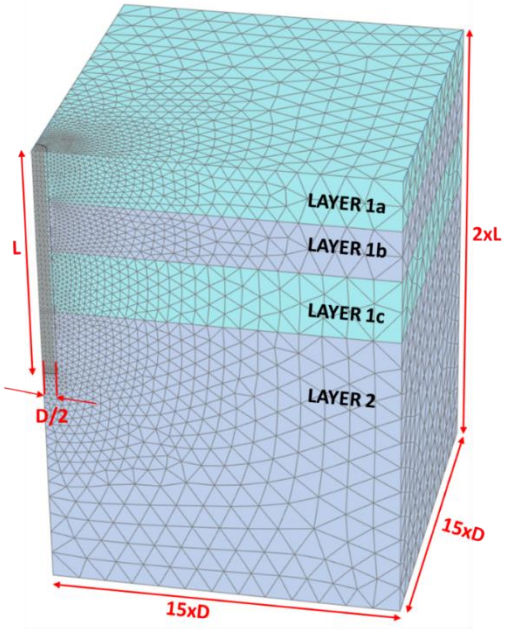

Fig. 2. Finite element mesh used in the simulations (single pile, D = 0.8 m, L = 9 m)

The pile with diameter D is modeled by volume elements with material properties of concrete. An elasto-plastic contact was implemented between pile and the adjacent soil. The maximum shear stresses in the contact surface (τ_{max}) result from the product of the horizontal stresses (σ_H) and the contact friction angle (δ), which was assumed in the range of 70% - 85% of the friction angle (φ').
The simulation is done in several steps. In the first step, the initial stress state is generated by consideration of soil elements only: the horizontal stresses (σ_H) are defined by a coefficient of horizontal earth pressure at rest (k_0).
Subsequently, the predefined elements defining the pile geometry are replaced by concrete elements with a linear-elastic material law (wished-in-place procedure). In the same step, the contact between the pile and the surrounding soil is activated. In a third step, the vertical load of $N = N_{serv,0}$ is applied to the center of the pile and finally, the center of the pile is loaded until a settlement, equal to 10% of the pile diameter, is reached.
To model the soil's material behavior, the HSsmall model according to Benz (Benz, 2006) was used. This soil model is an upgrade of the sophisticated Hardening Soil Model according to Schanz (Schanz, 1998) which enables for instance the consideration of the stress-dependency of soil stiffness. The HSsmall model is additionally able to account for the strain dependency of soil stiffness, being crucial for the response to small loads.
The formulation of the material law and the meaning of the required parameters is explained in detail in the user manual of PLAXIS3D (Brinkgreve et al., 2018) and is not further explained in this article.

3.3 Interaction pile – micropiles

As previously explained, an extended numerical model was used to evaluate the load bearing behavior of the reinforced foundation. The reinforcement consists in a group of four self-drilling micropiles, symmetrically arranged around each cast-in-place

bored pile, with an inclination of 15° (referred to the vertical axis). A concrete pile cap (2.4 m x 2.4 m x 0.8 m) was modelled to generate a rigid connection between the bored pile and the micropiles.
The calculation is done in five steps, as schematically presented in Fig. 3.

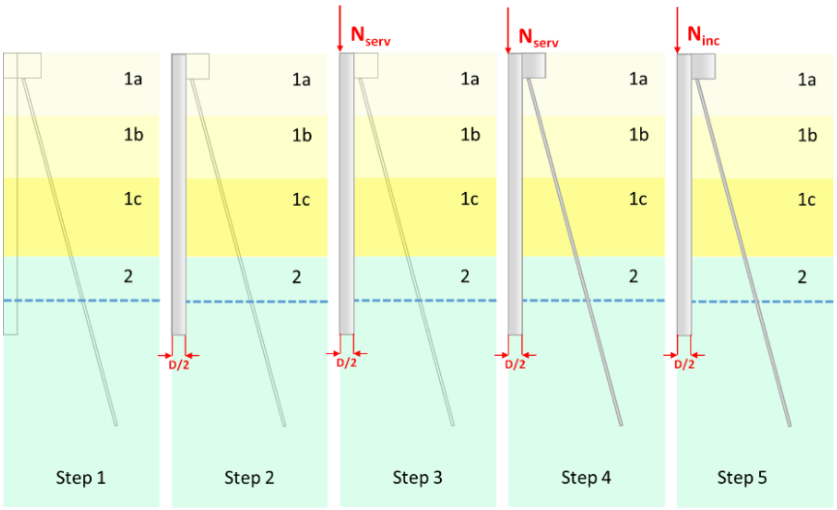

Fig. 3. Schematic presentation of the calculation steps for the system reinforced by micropiles

In the numerical simulation, the first three steps are similar to the single-pile model. In a fourth step, the predefined elements representing the micropile and the rigid pile cap are activated. In the last step, an incremental vertical load ($\mathbf{N_{inc}}$) is applied to the center of the pile cap until a settlement, equal to 10% of the pile diameter (**D**), is reached (Fig. 3).

4. PARAMETRIC STUDY

For the present study, three different ground conditions with different geotechnical properties were assigned to the load bearing stratum (Layer 2, Fig. 4): medium dense to dense gravels for Case 1, medium dense sands for Case 2 and firm to stiff clays for Cases 3 and 4, respectively.

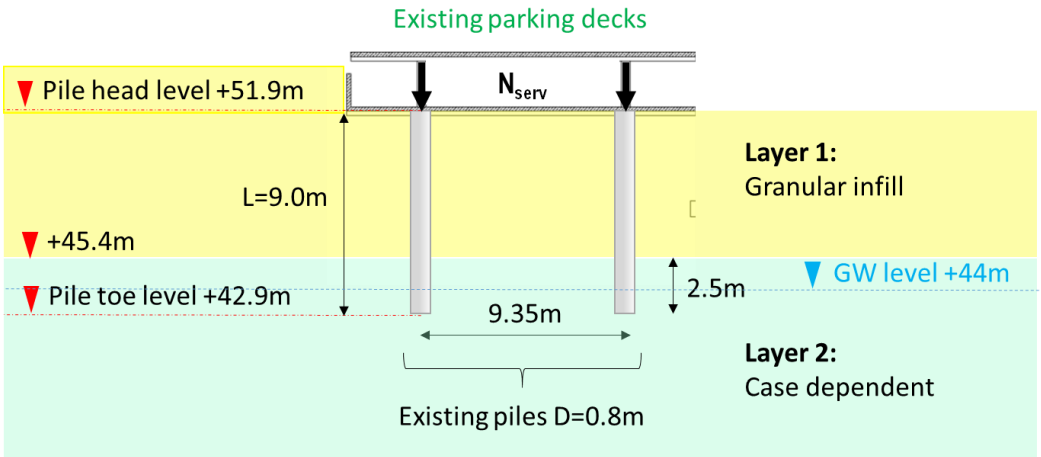

Fig. 4. Adopted configuration for the parametric study

For each case, the pile geometry (D = 0.8m and L = 9.0 m) and the parameters of the granular infill (Layer 1) were kept constant, varying only the geotechnical parameters of the load bearing stratum (Layer 2) and the (initial) loading magnitudes ($\mathbf{N_{serv,0}}$).

4.1 Definition of the initial loading ($N_{serv,0}$)

The initial pile loadings ($\mathbf{N_{serv,0}}$) have been obtained from the evaluation of the load bearing behavior of the single piles according to the analytical model of the EAP (DGGT, 2012), in a way that their values do not exceed the admissible load ($\mathbf{R_{allow}}$), calculated considering a typical safety factor **FS = 2.0**. For the analytical evaluation, the parameters listed in Table 2 were adopted.

Table 2. Adopted parameters for the existing piles according to (DGGT, 2012)

Case	Layer	Description	CPT - Tip resistance q_c (MN/m²)	Undrained shear resistance c_{uk} (kN/m²)	Base pressure $q_{b,k}$ (kN/m²)			Skin friction $q_{s,k}$ (kN/m²)
					s/D= 0.02	s/D= 0.03	s/D= 0.10	
1 - 4	1	Granular infill, loose	2	-	-	-	-	15
1	2	Gravels, med. dense to dense	14	-	983	1263	2813	98
2	2	Sands, med. dense	11	-	717	917	2067	72
3 - 4	2	Clays, firm - stiff	-	150	600	700	1200	50

The results of the analysis are presented as load-settlement curves for the four cases in the following Figures, with a close-up of the highlighted area, corresponding to settlements up to s = 2.0 cm.
Based on the load-settlement curves calculated with the analytical EAP approach, an initial loading **$N_{serv,0}$ = 1000 kN** was adopted for Case 1, **$N_{serv,0}$ = 850 kN** for Case 2, and **$N_{serv,0}$ = 550 kN** for Cases 3 and 4. The corresponding settlements are **s ≈ 0.8 cm** for Case 1, **s ≈ 0.8 cm** for Case 2 and **s ≈ 0.6 cm** for Cases 3 and 4.

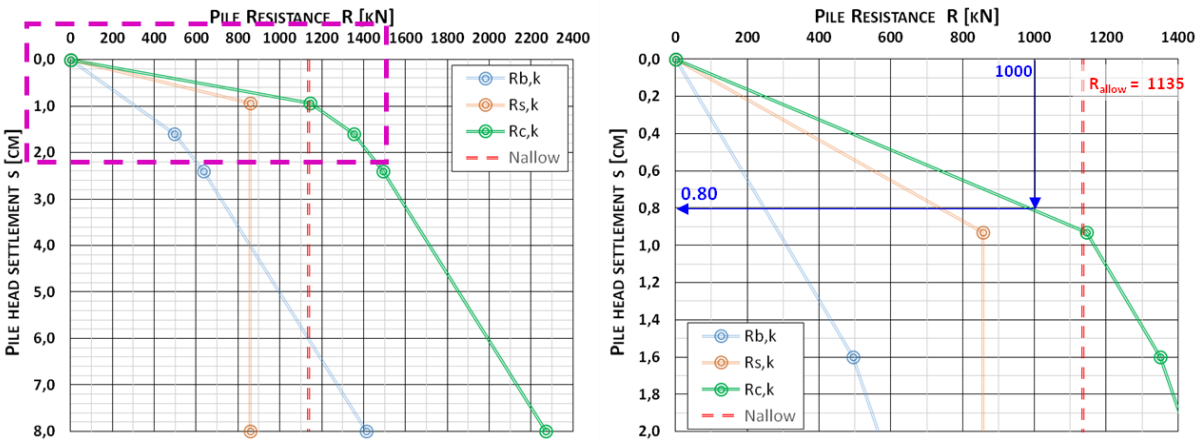

Fig. 5. Load - settlement curves from the analytical model (Case 1)

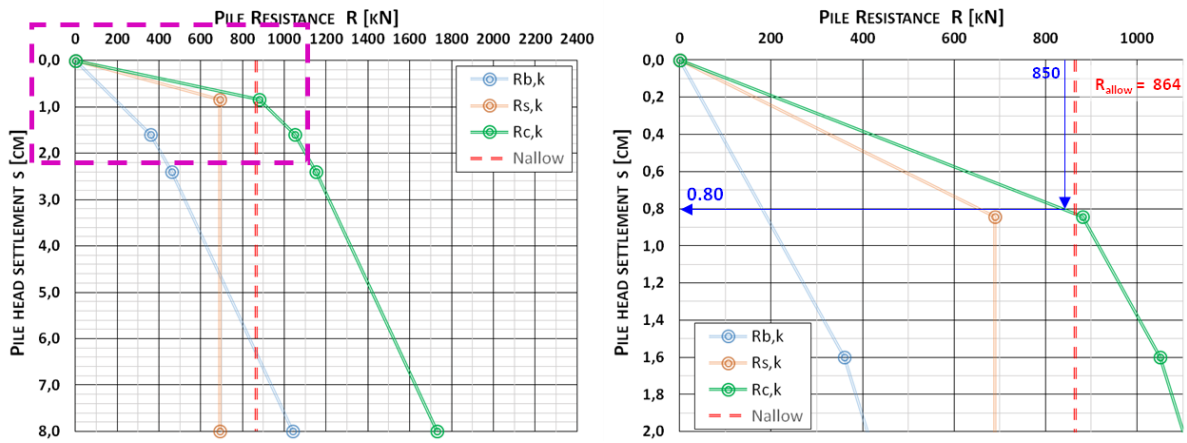

Fig. 6. Load - settlement curves from the analytical model (Case 2)

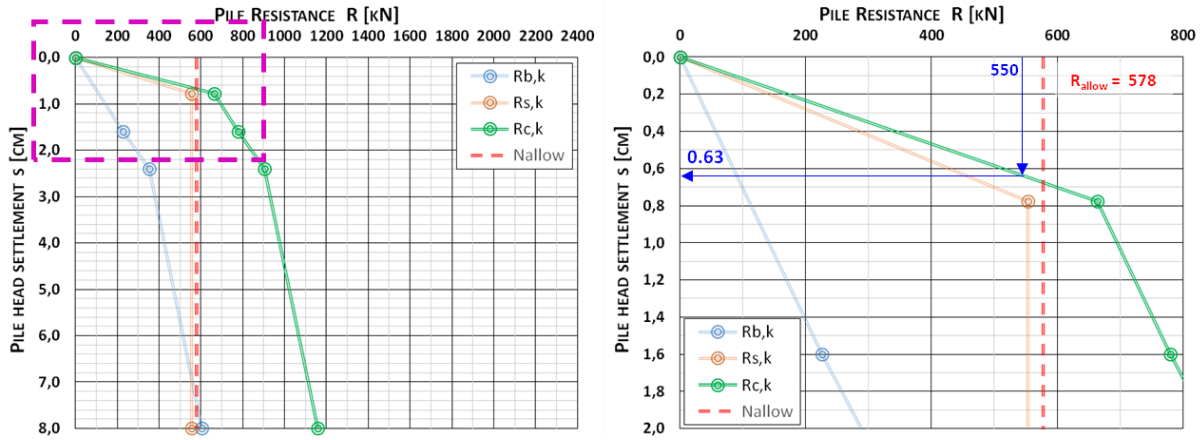

Fig. 7. Load - settlement curves from the analytical model (Case 3 and 4)

4.2 Numerical simulations

With the initial pile loading **($N_{serv,0}$)** obtained for all the analysis cases, the numerical simulations were conducted, as described in sections 2.2 and 2.3.

The soil properties have been chosen on basis of the Plaxis recommendations and the Recommendations of the Committee of Soil Dynamics (DGGT, 2003) with slight modifications in order to fit the FEM results to the load-displacement curves of the analytical approach, as described previously in sections 2.1 and 3.1 (Fig. 5 to 7).

PLAXIS 3D allows the execution of an undrained analysis with the use of effective stiffness parameters by considering the high stiffness of the water in the pores (**K_w**) in the assembly of the stiffness matrices (Undrained A-Method). Herein, the following connection between the increments of pore water pressure (**Δp_w**) and volume strain (**$\Delta \varepsilon_v$**) are assumed (Brinkgreve et al., 2018):

$$\Delta p_w = {}^{K_w}/_{n} * \Delta \varepsilon_v \qquad [5]$$

Here n is the soil's porosity. Using the Undrained A method in Plaxis, the effective shear strength parameters φ' and c' listed in Table 3 (Cases 3 and 4) were adopted to simulate the undrained shear resistance (**$c_{u,k}$**) defined in Table 2 for the firm-stiff clays (Layer 2). The following tables present the adopted parameters for the simulations:

Table 3. Soil parameters used in the simulations – Material law: HSsmall

Case	1 - 4			1	2	3 – 4
Layer	1a	1b	1c	2	2	2
Upper level (m)	0.0	-2.0	-4.0	-6.5	-6.5	-6.5
Description	Granular infill, loosen			Gravels, dense	Sands, med. dense	Clay, firm-stiff
Unit weight (effective): γ' (kN/m^3)	8.8	8.8	8.8	11.5	10.3	8.5
Initial void ratio: e_{init} (-)	0.85	0.85	0.85	0.60	0.6	0.5
Secant triaxial loading stiffness: E_{50}^{ref} (kN/m^2)	1452	3497	5471	57360	32580	10000
Tangent oedometer loading stiffness: E_{oed}^{ref} (kN/m^2)	1177	2835	4436	57360	32580	10000
Triaxial unloading/reloading stiffness: E_{ur}^{ref}(kN/m^2)	4356	10490	16414	225434	102467	30000
Exponent: m (-)	0.8	0.8	0.8	0.5		
Cohesion: c' (kN/m^2)	0.1	0.1	0.1	0.1	0.1	70
Friction angle: φ' (°)	28	28	28	40	38	20
Dilatancy: ψ (°)	0	0	0	2	3	0
Reference shear strain: $\gamma_{0.7}$ (-)	1x10^{-4}			1x10^{-4}	1x10^{-4}	1x10^{-4}
Dynamic shear modulus: G_0^{ref} (kN/m^2)	19652	34035	45023	107545	80000	28000
Poisson's ratio: μ (-)	0.3			0.2	0.25	0.3
Reference stress: p_{ref} (kN/m^2)	6.05	18.14	31.74	73.27	71.91	89.92
At-rest earth pressure coefficient: k_0 (-)	0.531	0.531	0.531	0.357	0.384	0.658
Reduction factor for interfaces R_{inter} (-)	0.75			0.85	0.85	0.7

Table 4. Bored pile parameters used in the simulations – Material law: Linear-elastic

Structural element	Bored pile
Case	1-4
Upper level (m)	0.0
Length (m)	9.0
Diameter: D (m)	0.8
Unit weight: γ (kN/m^3)	25
Young's modulus: E (kN/m^2)	30x10^6
Poisson's ratio: ν (-)	0.2

Table 5. Micropiles parameters used in the simulations – Material law: Linear-elastic

Structural element	Embedded pile (skin friction only)					
Case	1 - 3	4	1	2	3	4
Total length: L_{tot} (m)	--		12	12	12	15
Layer	1		2	2	2	
Upper level (m)	0.0		-6.5	-6.5	-6.5	
Unit weight (effective): γ' (kN/m^3)	25					
Young's modulus: E (kN/m^2)	30×10^6					
Length in layer: L_i (m)	6.7		5.3	5.3	5.3	8.3
Shaft diameter: d (cm)	15	17	15	15	17	17
Skin friction: τ_{max} (kN/m)	33	37	120	90	53	53

The only difference between Case 3 and Case 4 resides in the length of the considered reinforcing micropiles (Table 5).

4.3 Evaluation of the numerical simulation results for the single bored piles

The results of the numerical analysis of the single piles are presented in Fig. 8 in terms of load-settlement curves. The results for the analytical approach are depicted for comparison.

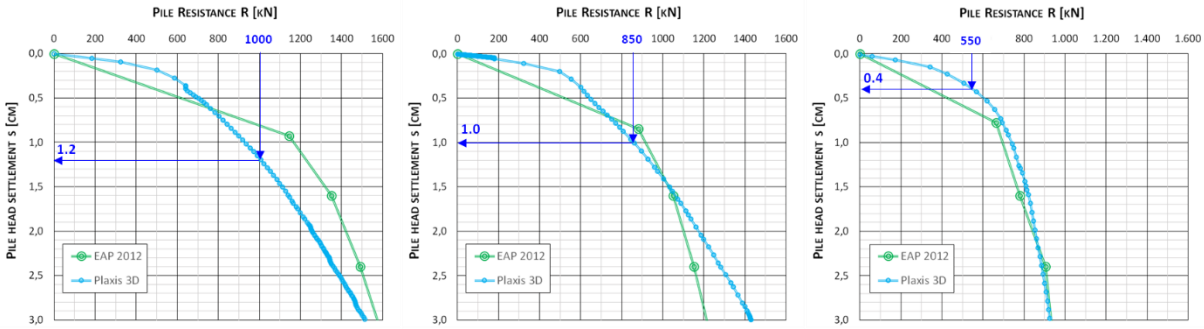

Fig. 8. Comparison of the analytical and numerical results for the single bored piles

Based on the resistance behavior simulated by the numerical models, a settlement **s ≈ 1.2 cm** was obtained for the initial loading ($\mathbf{N_{serv,0}}$) of Case 1, **s ≈ 1.0 cm** for Case 2 and **s ≈ 0.4 cm** for Case 3, respectively.
There is a congruency in the mobilized pile resistances for settlements up to 3.0 cm, corresponding to 3.75% of the pile diameter (D). As expected, the numerical model presents a stiffer response for small settlements (<0.8 cm), consistent with the stiff soil behavior to be expected for small strains.
Due to the observed good agreement, the resistance behavior of the piled foundation, simulated by the numerical model, can be considered suitable for the subsequent analysis of the reinforcement and its interaction with the existing piles.

4.4 Evaluation of the results for the reinforced foundations

The resistance of the foundation ($\mathbf{R_{Foundation}}$) shall be taken here -for design purposes- as the lesser of the following values:

- the admissible load ($\mathbf{R_{allow}}$), considering a typical safety factor FS = 2.0.
- the load corresponding to a maximal settlement s_{max} = 2.0 cm ($\mathbf{R_{s=2.0}}$)

4.4.1 Case 1

In case 1, embedment of the piles in a very stiff gravel layer is considered. The calculated load-displacement curve for the foundation is presented in Fig. 9. With regard to factor of safety, the reinforced foundation (bored pile and micropiles) has an admissible load of $\mathbf{R_{allow} = 3400\ kN}$. However, here the settlement criterion is decisive and leads to a foundation resistance $\mathbf{R_{Foundation} = R_{s=2.0} = 3200\ kN}$.

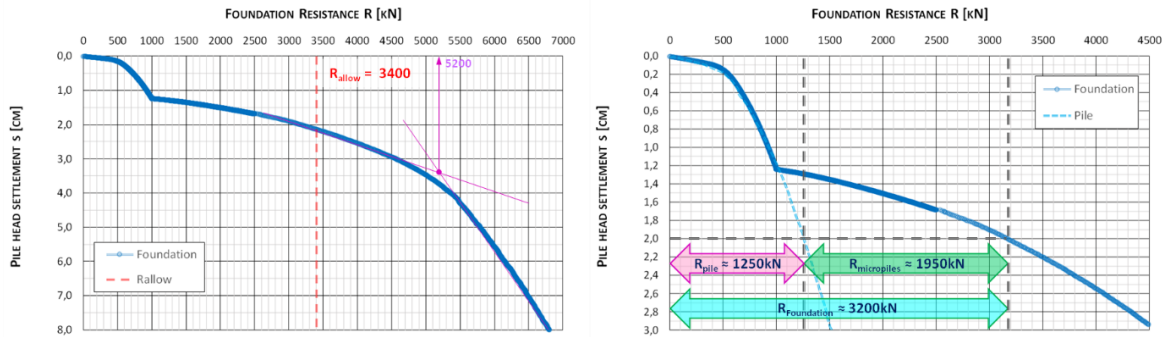

Fig. 9. Results of the numerical analysis (Case 1)

The resistance-settlement diagram shows that there is a slight change in the curvature of the diagram at a load level of approx. 5200 kN (Fig. 9, left), which suggests that the foundation stiffness begins to decrease, most likely because the mobilized skin friction of the reinforcing micropiles is reaching its maximum capacity.
A close-up of the resistance-settlement diagram (Fig. 9, right) shows that the reinforced foundation is able to resist approx. 3.2-times the initial loading $\mathbf{N_{serv,0} = 1000\ kN}$, making the contribution of the micropiles evident.
Due to the rigid connection between the different elements, the settlements of the reinforced foundation are also induced to the bored pile. For the above mentioned limit settlement of $\mathbf{s = 2.0\ cm}$, the bored pile would mobilize a resistance of $\mathbf{R_{pile} = 1250\ kN}$, and the micropiles $\mathbf{R_{micropiles} = 1950\ kN}$, respectively.

4.4.2 Case 2

The analysis results for case 2 (pile embedment in a sand layer) are presented in Fig. 10. Based on a safety factor of 2.0, the reinforced foundation (bored pile and micropiles) has a resistance $\mathbf{R_{Foundation} = 2850\ kN}$. The settlement criterion here yields a greater admissible load ($\mathbf{R_{s=2.0} = 3000\ kN}$).
Similar to Case 1, the resistance-settlement curve generates the maximum skin friction of the micropiles at approx. 4200 kN (Fig. 10, left).

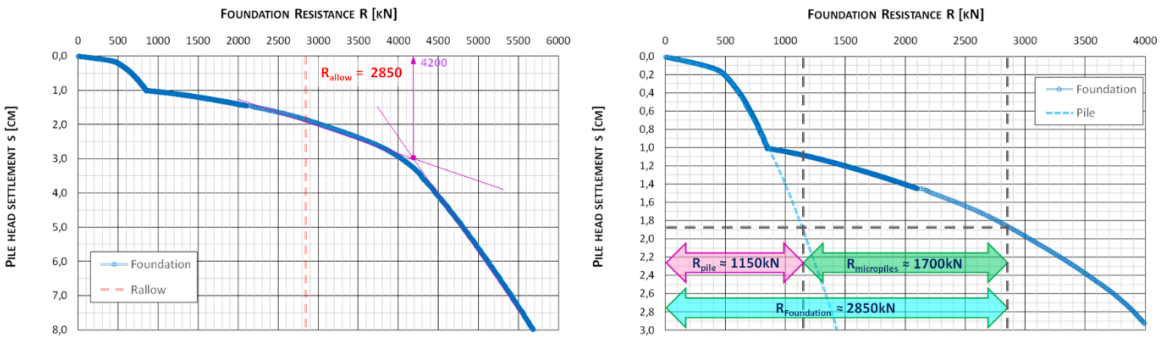

Fig. 10. Results of the numerical analysis (Case 2)

In Case 2, the reinforced system is able to withstand approx. 3.35-times the initial loading $\mathbf{N_{serv,0} = 850\ kN}$ based on the contribution of the micropiles. To mobilize the above mentioned allowable resistance ($\mathbf{R_{allow}}$), a settlement of $\mathbf{s = 1.9\ cm}$ is necessary, at which the bored pile mobilizes a resistance of $\mathbf{R_{pile} = 1150\ kN}$ and the micropiles $\mathbf{R_{micropiles} = 1700\ kN}$.

4.4.3 Case 3

In case 3, the embedment of the piles in a firm to stiff clay layer and a micropile length of 12 m are considered. The analysis results are presented in Fig. 11. The reinforced foundation (bored pile and micropiles) has a resistance $\mathbf{R_{Foundation} = 1900\ kN,}$ corresponding to the admissible resistance with respect to factor of safety ($\mathbf{R_{allow}}$).
Compared with the previous cases, the resistance-settlement diagram shows that there is a more evident change in the curvature of the diagram at a load level of approx. 2900 kN (Fig. 11, left), which suggests that the foundation stiffness decays considerably, most likely because the mobilized skin friction of the reinforcing micropiles is close to its ultimate capacity.
According to the resistance-settlement diagram (Fig. 11, right), the reinforced foundation is able to resist approx. 3.45-times the initial loading $\mathbf{N_{serv,0} = 550\ kN}$. For the mutual bearing mechanism of the bored pile and micropile in order to mobilize the above mentioned allowable resistance ($\mathbf{R_{allow}}$), a settlement of $\mathbf{s = 0.9\ cm}$ is needed. Hence, the bored pile generates $\mathbf{R_{pile} = 700\ kN}$, and the micropiles $\mathbf{R_{micropiles} = 1200\ kN}$, respectively.

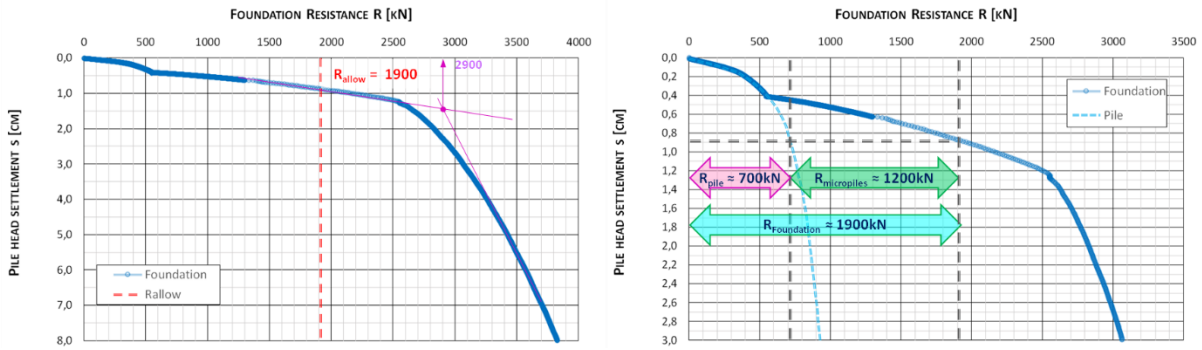

Fig. 11. Results of the numerical analysis (Case 3)

4.4.4 Case 4

Case 4 is identical to case 3, but a length of the micropiles of 15 m is considered. The analysis results are presented in Fig. 12. The reinforced foundation (bored pile and micropiles) has a resistance $\mathbf{R_{Foundation} = 2200kN,}$ corresponding as for case 3 to the admissible resistance ($\mathbf{R_{allow}}$) with respect to factor of safety.
The change in the curvature in the resistance-settlement diagram happens at a load level of approx. 3500 kN (Fig. 12, left).

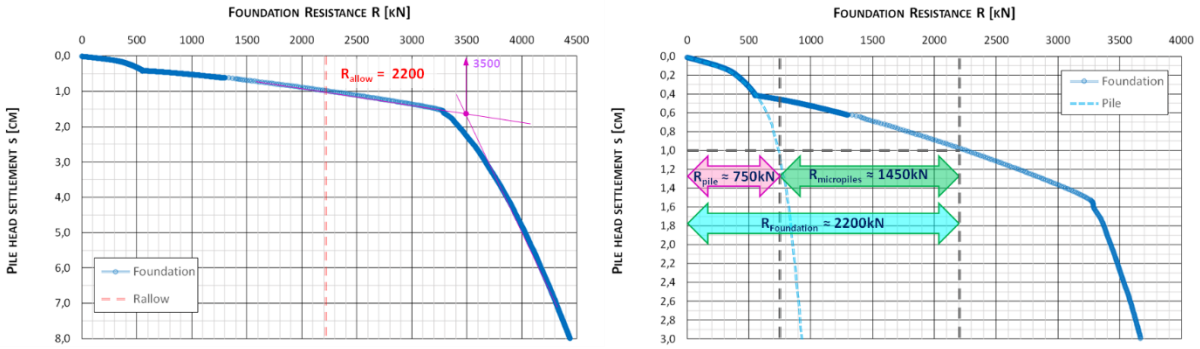

Fig. 12. Results of the numerical analysis (Case 4)

The diagram (Fig. 12, right) shows an increase in resistance of approx. 4.0-times the initial loading $\mathbf{N_{serv,0} = 550\ kN}$. The settlement of the reinforced foundation needs to be **s = 1.0 cm** in order to mobilize the above mentioned allowable resistance ($\mathbf{R_{allow}}$). The bored pile mobilizes a resistance of $\mathbf{R_{pile} = 750\ kN}$, and the micropiles $\mathbf{R_{micropiles} = 1450\ kN}$.

For both calculations in clay, no additional consolidation phase after (undrained) loading was considered. Taking this into account would lead to slightly greater settlements of both the single bored pile and the reinforced system. For instance, a consolidation of the single bored pile prior to the installation of the micropiles roughly leads to 0.3 cm additional settlement.

5. SUMMARY OF THE PARAMETRIC STUDY

For the present study, four cases were analyzed with a numerical model, where three different ground conditions with different geotechnical properties were assigned to the load bearing stratum (Fig. 4, Layer 2): medium dense to dense gravels for Case 1, medium dense sands for Case 2 and firm to stiff clays for Cases 3 and 4, respectively.
For each case, an initial loading was applied to the single pile. The magnitude of the initial loading was chosen to be as close to the admissible resistance as possible, obtained by applying a safety factor FS = 2.0 to the ultimate pile resistance, determined analytically according to the conventional design practice for piled foundations.
A reinforced foundation was then investigated, consisting of a group of four micropiles inclined by 15° to the vertical axis, symmetrically arranged around the original pile. An (almost rigid) connection of the bored pile and the micropiles by a reinforced concrete pile cap was assumed.
The results of the parametric study show that the micropiles can significantly improve the foundation resistance by increasing the admissible load to a load between 3.2

and 4.0-times higher than the value of the initial loading, applied to the single pile (without reinforcement).
The results of the analysis are summarized in the following Figure 13. The resistances of the reinforced foundations, compared to the resistances of the single piles (equal to the initial loading conditions) are presented in Fig. 13 (left). The loading distribution among the reinforced foundation elements (bored pile and micropiles) is shown in Fig.13 (right). The contribution of the micropiles to the load-bearing capacity of the reinforced foundation is evident, representing more than 60% of the total resistance.

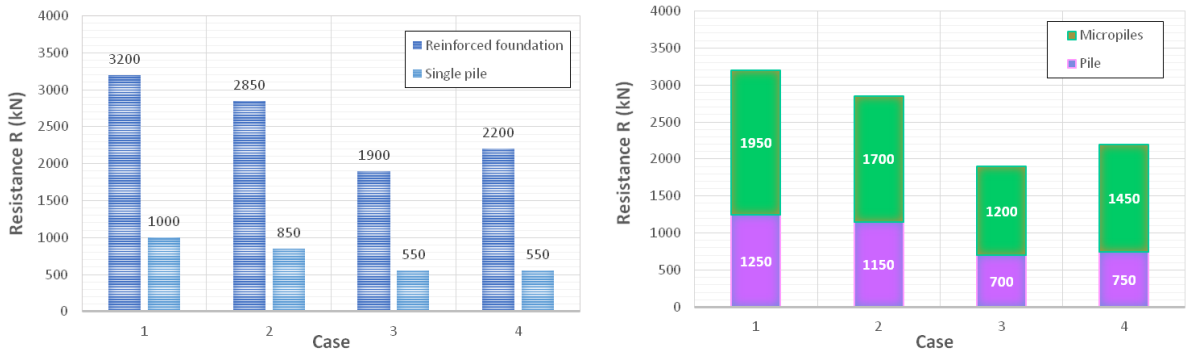

Fig. 13. Results of the analysis

It is worth mentioning, that the extended load bearing capacity requires only small additional settlements, which does not exceed a defined limit value for the total settlement of 2.0 cm, corresponding to the usually accepted range for settlements under service load. The load-bearing behavior of the reinforced foundation can be considered as completely satisfactory.
Finally, the constructive layout of the reinforced foundation is schematically presented in Fig. 14.

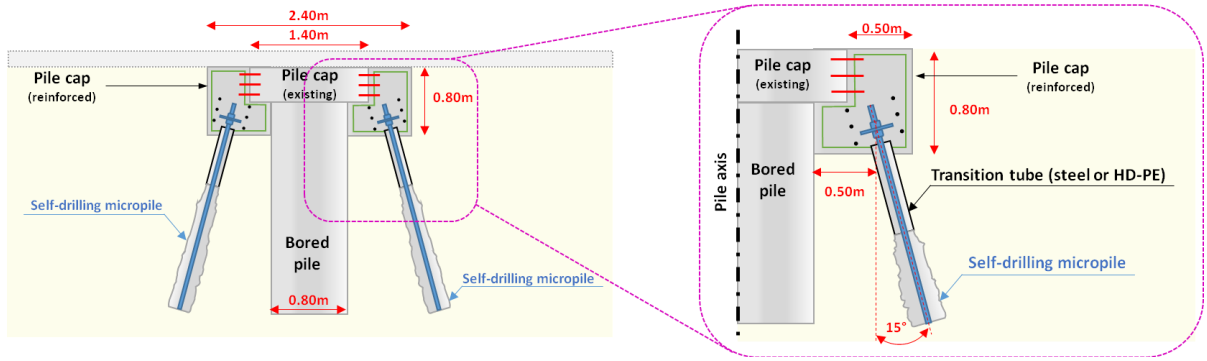

Fig. 14. Schematic layout of the reinforced foundation

6. REFERENCES

Benz, T., 2006. *Small Strain Stiffness of Soils and its Numerical Consequences*, Ph.D. thesis, University of Stuttgart.

Brinkgreve, R.B.J., Engin, E., Swolfs, W.M., 2018. *PLAXIS 3D 2018 Manual*.

Deutsche Gesellschaft für Geotechnik (DGGT), 2003. *Empfehlungen des Arbeitskreises „Baugrunddynamik“*, Ernst & Sohn, p. 200.

Deutsche Gesellschaft für Geotechnik (DGGT), 2012. *Empfehlungen des Arbeitskreises „Pfähle"* (EAP), Ernst & Sohn, p. 498.

European Standard EN 1997-1: *Eurocode 7, Geotechnical Design – Part 1: General Rules*, 2010.

Lopez, F., Fernandez, J.M., 2017. *Edificio Piedra Real – Concepcion, Chile. Case study of an uplift reinforcement project*. Proceedings of the 13th International Workshop on Micropiles, Vancouver, March 29-April 1.

Lopez, F., Severi, G., 2018. *Micropiling in Urban Infrastructure: Advantages, Experience and Challenges*. Proceedings of the DFI-EFFC International Conference on Deep Foundations and Ground Improvement, Rome, June 5-8.

Lopez, F., Terceros, M., Achmus, M., 2018. *Reinforcement of Existing Deep Foundations with Micropiles*. Proceedings of the 43rd DFI Annual Conference, Anaheim, October 24-27.

Schanz, T., 1998. *Zur Modellierung des mechanischen Verhaltens von Reibungsmaterialien*, Habilitation, University of Stuttgart (in German).